European Journal of Radiology 118 (2019) 114–121

Contents lists available at ScienceDirect

European Journal of Radiology

journal homepage: www.elsevier.com/locate/ejrad

Complete response on MR imaging after neoadjuvant chemotherapy in breast cancer patients: Factors of radiologic-pathologic discordance

Woo Jung Choi, Hak Hee Kim*, Joo Hee Cha, Hee Jung Shin, Eun Young Chae, Ga Young Yoon

Department of Radiology and Research Institute of Radiology, Asan Medical Center, University of Ulsan College of Medicine, 88, Olympic-ro 43-gil, Songpa-gu, Seoul 05505, Republic of Korea

ARTICLE INFO

Keywords:
Breast cancer
Chemotherapy
Magnetic resonance imaging
Mammography
Ultrasound

ABSTRACT

Purpose: To evaluate the radiologic and clinicopathologic factors in radiologic-pathologic discordance (false-negative results) in breast cancer patients who demonstrate radiologic complete response (rCR) in MR imaging after neoadjuvant chemotherapy (NAC).

Method: Our institutional review board approved this retrospective study. We included 209 consecutive patients who showed rCR in MR imaging after NAC. rCR was diagnosed when the original lesion site showed no enhancement. Pathologic CR (pCR) was defined as the complete absence of both invasive cancer and ductal carcinoma in situ in the breast upon pathology. Clinicopathologic and radiologic factors affecting the radiologic-pathologic correlation were analyzed.

Results: pCR was noted in 108 patients (51.7%); the remaining 101 (48.3%) had residual lesion on pathology. False negative rCR findings were significantly more frequent in cases of 1 or 2 histologic grade ($p = 0.001$), low tumor-infiltrating lymphocytes ($p = 0.004$), and luminal A or B subtype ($p < 0.001$). Multivariate analysis of radiologic findings to identify predictors of false negative findings found calcifications in mammography ($p = 0.037$), multifocal multicentric lesions ($p = 0.004$), and non-mass enhancement in pretreatment MR imaging ($p = 0.023$) to be significantly associated with false-negative findings.

Conclusions: Patients with calcification in mammography, multifocal multicentric lesions, and non-mass enhancement in pretreatment MR imaging are significantly associated with false-negative results who showed rCR on MR imaging after NAC. These patient populations should be interpreted with caution.

1. Introduction

Neoadjuvant chemotherapy (NAC) is a standard-of-care for patients with locally advanced breast cancer and it is increasingly being used for patients with operable cancer [1–3]. NAC may reduce tumor size and increase the likelihood of breast-conserving surgery, while in cases of complete response, it would potentially reduce or eliminate surgical intervention [4,5]. In fact, a pathologic complete response (pCR) after NAC is consistently associated with a favorable prognosis [6–8]. Therefore, predicting both tumor response and residual tumor is important for developing a treatment plan and evaluating prognosis.

Mammography, breast ultrasound (US), and contrast-enhanced magnetic resonance (MR) imaging are commonly used for evaluating the extent of the tumor before and after NAC. Because it allows characterization of tumor angiogenesis, contrast-enhanced imaging is considered the most effective imaging technique for monitoring the tumor response, as well as assessing residual disease after NAC. Despite the high accuracy of MR imaging [9–13], there are still problems with false positive and false-negative results [10,14–16]. Moreover, although mammographically identified residual microcalcifications do not always correlate with residual tumor burden, MR imaging has a limited ability to accurately evaluate the extent of malignant microcalcifications, which require complete excision [17]. Recent studies investigated the use of minimally invasive biopsy to overcome this diagnostic challenge [18–20], but the hypothesis remains controversial. With all these concerns, preoperative imaging is still important for predicting tumor response. In addition, although MR imaging has been the most effective imaging tool, mammography may also have an important role especially in patients with microcalcifications.

Therefore, the purpose of this study was to evaluate the radiologic and clinicopathologic factors affecting the potential for radiologic-pathologic discordance in breast cancer patients demonstrating radiologic

* Corresponding author.
E-mail addresses: wjc@amc.seoul.kr (W.J. Choi), hhkim@amc.seoul.kr (H.H. Kim), jhcha@amc.seoul.kr (J.H. Cha), docshin@amc.seoul.kr (H.J. Shin), chaeey@hanmail.net (E.Y. Chae), 3770ghwo@hanmail.net (G.Y. Yoon).

https://doi.org/10.1016/j.ejrad.2019.06.017
Received 28 March 2019; Received in revised form 17 June 2019; Accepted 20 June 2019

complete response (rCR) on MR imaging after NAC.

2. Materials and methods

Our hospital's institutional review board approved this retrospective study and the requirement for informed patient consent was waived.

2.1. Study population

From January 2013 through December 2015, 250 consecutive female patients with locally advanced breast cancer and rCR on MR imaging performed after NAC, but prior to surgery were included. All patients underwent mammography, as well as US and MR imaging before and after NAC. rCR was diagnosed when either no enhancement was found in the original lesion site in any of the MR images after completion of NAC. Exclusion criteria included: diagnosis and pretreatment MR imaging performed at a different institution without recorded information on the use of a computer-aided diagnosis (CAD) system; bilateral breast cancer; distant metastasis at the time of diagnosis; underwent neoadjuvant endocrine therapy. After applying these criteria, a total of 209 patients (mean age, 49 years; range, 24–76 years) were included in this study. The mean interval between the first MR examination and treatment was 12 days (range, 2–29 days), and second MR examination and surgery was 11 days (range, 1–27 days).

2.2. Image acquisition and analysis

Mammography was obtained using a full-field digital mammography system (Senographe DS; GE Healthcare, Milwaukee, WI, USA). Whole-breast US was performed by board-certified radiologists with 1–23 years of breast US experience using an IU22 (Philips Healthcare, Bothell, WA), equipped with a 50-mm linear-array transducer with a bandwidth of 7–12 MHz. Breast MR imaging was performed using either a 1.5 T (Avanto; Siemens Medical Solutions, Erlangen, Germany) or 3 T MR scanner (Ingenia; Philips, Best, The Netherlands, or Skyra; Siemens Medical Solutions, Erlangen, Germany), and a dedicated, 18-channel phased-array breast coil (Siemens Medical Solutions). The MR imaging protocol was performed using the following imaging parameters (1.5 T, 3 T): an axial short inversion time inversion-recovery (STIR) sequence (repetition time [TR]/echo time [TE], 1300/131, 5722/4.1 ms; field of view, 340 × 340, 320 × 320 mm^2; matrix size, 448 × 448, 512 × 512; slice thickness, 1.5, 2 mm), as well as a pre- and postcontrast-enhanced fat-saturated axial three-dimensional T1-weighted fast low-angle shot (FLASH) dynamic gradient-echo sequence (TR/TE, 5.0/2.4, 4.1/1.8 ms; field of view, 340 × 340, 337 × 337 mm^2; matrix size, 384 × 384, 384 × 384), with a temporal resolution of 61 s. The dynamic contrast-enhanced MR images were acquired before and after a bolus of 0.1 mmol/kg gadopentetate dimeglumine (UNIRAY®, Dongkook Pharmaceutical Co., Ltd, Seoul, Korea), injected at a flow rate of 2 ml/s using an MR-compatible power injector (Spectris; Medrad, Pittsburgh, PA, USA). Each contrast material injection was followed by a 20-ml saline flush. All T1-weighted images were transferred to a commercially available CAD system (CADSTREAM, version 6.0.1; Confirma, Kirkland, WA), which automatically calculated tumor diameter, angio volume (total enhancing lesion volume), peak enhancement (highest pixel signal intensity in the first post-contrast series), and delayed enhancement (proportions of persistent, plateau, and washout-enhancing components) [21,22]. The persistent type indicated increased pixel signal intensity of > 10% from the first postcontrast series. The plateau type indicated increased pixel signal intensity in the last postcontrast series of < 10% and decreased intensity of < 10% from the first postcontrast series. The washout type indicated decreased pixel signal intensity in the last postcontrast series of > 10% from the first postcontrast series.

All images were reviewed by two dedicated breast radiologists (W.J.C and H.H.K., with 7 and 27 years of experience in breast imaging, respectively) in consensus. Pretreatment imaging features were described according to the American College of Radiology's BI-RADS 5th protocols [23]. Mammographic findings were evaluated for breast parenchymal density and type of lesion (with/without calcification). Masses were described by shape, margin, and density. When calcifications were present, the mammograms taken before and after NAC were reviewed with regard to morphologic features and distribution, and the changes between them were evaluated. US images were evaluated for the presence or absence of a mass; identified masses were described by shape, orientation, margin, echo pattern, and posterior acoustic features. For breast MR images, background parenchymal enhancement and type of lesion (mass, non-mass enhancement) were analyzed. Masses were described by shape, margin, internal enhancement, peritumoral edema, and intratumoral high signal intensity on T2-weighted imaging. Non-mass enhancement was described by its distribution and internal enhancement. Multifocal or multicentric status and CAD-generated kinetics were also reviewed.

Table 1
Clinicopathologic features of 209 patients treated with neoadjuvant chemotherapy correlated with pathological response.

	All patients	pCR (n = 108)	False negative (n = 101)	P value
Age (y)*	49.0 ± 9.6	49.2 ± 9.6	48.7 ± 9.7	0.671
Clinical stage at diagnosis				0.107
IIA	57 (27.3)	36 (33.3)	21 (20.8)	
IIB	74 (35.4)	34 (31.5)	40 (39.6)	
IIIA	30 (14.3)	17 (15.7)	13 (12.9)	
IIIB	2 (1.0)	0 (0)	2 (2.0)	
IIIC	46 (22.0)	21 (19.5)	25 (24.7)	
Neoadjuvant chemotherapy regimen				0.510
Anthracycline-based	18 (8.6)	11 (10.2)	7 (6.9)	
Anthracycline- and taxane-based	178 (85.2)	89 (82.4)	89 (88.1)	
HER2-targeted	13 (6.2)	8 (7.4)	5 (5.0)	
Histologic grade				< 0.001
1	3 (1.4)	1 (0.9)	2 (2.0)	
2	122 (58.4)	49 (45.4)	73 (72.3)	
3	84 (40.2)	58 (53.7)	26 (25.7)	
Tumor-infiltrating lymphocytes				0.004
Low (0–50)	93 (60.8)	38 (49.4)	55 (72.4)	
High (> 50)	60 (39.2)	39 (50.6)	21 (27.6)	
Estrogen receptor				< 0.001
Negative	107 (51.2)	74 (68.5)	33 (32.7)	
Positive	102 (48.8)	34 (31.5)	68 (67.3)	
Progesterone receptor				< 0.001
Negative	145 (69.4)	92 (85.2)	53 (52.5)	
Positive	64 (30.6)	16 (14.8)	48 (47.5)	
HER2				0.762
Negative	114 (54.5)	60 (55.6)	54 (53.5)	
Positive	95 (45.5)	48 (44.4)	47 (46.5)	
Ki-67				0.002
Low (< 14%)	31 (14.8)	8 (7.4)	23 (22.8)	
High (≥14%)	178 (85.2)	100 (92.6)	78 (77.2)	
Molecular subtype				< 0.001
Luminal A	14 (6.7)	1 (0.9)	13 (12.9)	
Luminal B	89 (42.6)	34 (31.5)	55 (54.5)	
HER2-positive	49 (23.4)	27 (25.0)	22 (21.8)	
Triple-negative	57 (27.3)	46 (42.6)	11 (10.9)	
Surgery type				< 0.001
Breast-conserving surgery	136 (65.1)	83 (76.9)	53 (52.5)	
Mastectomy	73 (34.9)	25 (23.1)	48 (47.5)	

Note: Except were indicated, data are number of patients, with percentages in parentheses. HER2 = human epidermal growth factor receptor 2, pCR = pathologic complete response.

* Data are means ± standard deviations.

Table 2
Assessment of pretreatment mammographic features and changes in calcifications correlated with pathological response.

	All patients	pCR	False negative	P value
Density				0.432
Fatty	31 (14.8)	14 (13.0)	17 (16.8)	
Dense	178 (85.2)	94 (87.0)	84 (83.2)	
Type of lesion				0.002
Without calcification	124 (59.3)	75 (69.4)	49 (48.5)	
With calcification	85 (40.7)	33 (30.6)	52 (51.5)	
Mass shape				0.020
Oval or round	33 (17.8)	23 (24.2)	10 (11.1)	
Irregular	152 (82.2)	72 (75.8)	80 (88.9)	
Mass margin				0.113
Circumscribed	3 (1.6)	0 (0)	3 (3.3)	
Not circumscribed	182 (98.4)	95 (100)	87 (96.7)	
Mass density				> 0.999
High	171 (92.4)	88 (92.6)	83 (92.2)	
Equal	14 (7.6)	7 (7.4)	7 (7.8)	
Calcification morphology before NAC				0.201
Amorphous or coarse heterogeneous	42 (49.4)	19 (57.6)	23 (44.2)	
Fine pleomorphic, fine-linear or fine-linear branching	43 (50.6)	14 (42.4)	29 (55.8)	
Calcification distribution before NAC				0.357
Diffuse, regional, or grouped	59 (69.4)	21 (63.6)	38 (73.1)	
Linear or segmental	26 (30.6)	12 (36.4)	14 (26.9)	
Calcification changes after NAC				0.660
No change	54 (63.5)	23 (69.7)	31 (59.6)	
Increased	8 (9.4)	2 (6.1)	6 (11.5)	
Decreased	23 (27.1)	8 (24.2)	15 (28.9)	
Calcification morphology after NAC				0.218
Amorphous or coarse heterogeneous	47 (55.3)	21 (63.6)	26 (50)	
Fine pleomorphic, fine-linear or fine-linear branching	38 (44.7)	12 (36.4)	26 (50)	
Calcification distribution after NAC				0.357
Diffuse, regional, or grouped	59 (69.4)	21 (63.6)	38 (73.1)	
Linear or segmental	26 (30.6)	12 (36.4)	14 (26.9)	

Note: Data are number of patients, with percentages in parentheses. NAC = neoadjuvant chemotherapy, pCR = pathologic complete response.

Table 3
Assessment of pretreatment sonographic features correlated with pathological response.

	All patients	pCR	False negative	P value
Type of lesion				0.015
Mass	192 (91.9)	104 (96.3)	88 (87.1)	
Non-mass lesion	17 (8.1)	4 (3.7)	13 (12.9)	
Mass shape				0.173
Oval or round	39 (20.2)	25 (23.8)	14 (15.9)	
Irregular	154 (79.8)	80 (76.2)	74 (84.1)	
Mass orientation				0.885
Parallel	177 (91.7)	95 (90.5)	82 (93.2)	
Not parallel	16 (8.3)	10 (9.5)	6 (6.8)	
Mass margin				0.041
Obscured, microlobulated, or indistinct	149 (77.2)	87 (82.9)	62 (70.5)	
Spiculated	44 (22.8)	18 (17.1)	26 (29.5)	
Mass echo pattern				0.209
Hypoechoic	182 (94.3)	97 (92.4)	85 (96.6)	
Heterogeneous	11 (5.7)	8 (7.6)	3 (3.4)	
Mass posterior feature				0.184
No posterior features	76 (39.4)	39 (37.1)	37 (42.1)	
Enhancement	89 (46.1)	55 (52.4)	34 (38.6)	
Shadowing	13 (6.7)	5 (4.8)	8 (9.1)	
Combined pattern	15 (7.8)	6 (5.7)	9 (10.2)	

Note: Data are number of patients, with percentages in parentheses. pCR = pathologic complete response.

2.3. Histopathologic analysis

All patients underwent US-guided core biopsy before NAC and surgery after NAC, from which data were collected on the histologic type, nuclear and histologic grades, and immunohistochemical labeling of estrogen receptor (ER), progesterone receptor (PR), human epidermal growth factor receptor 2 (HER2) and Ki-67. Tumors subtypes included: luminal A (ER and/or PR positive, HER2 negative, Ki-67 < 14%); luminal B (ER and/or PR positive, HER2 negative and Ki-67 ≥ 14%; ER and/or PR positive, HER-2 overexpressed and/or amplified and any Ki-67); HER2-positive (ER and PR negative and HER2 overexpressed and/or amplified); and triple-negative (ER, PR, and HER2 negative) [24].

The histopathologic response of the tumor to NAC was assessed through examination of the tumor bed. pCR was defined as the complete absence of both invasive cancer and ductal carcinoma in situ in (DCIS) the breast upon surgical histopathological examination.

2.4. Statistical analysis

Clinicopathologic and pretreatment radiologic findings, post-treatment mammography with calcifications, and pathologic response data were assessed. False-negative results were defined as cases in which MR imaging data indicated rCR, but in which the surgical specimen did not meet pCR criteria. Statistical differences in continuous variables were assessed with analysis of variance, Kruskal–Wallis test or Student's t-test, while categorical variables were assessed by chi-square or Fisher's exact tests. Univariate and multivariate logistic regression analyses were performed to identify the features associated with false-negative findings. Variables with $P < 0.1$ were included in the multivariate analysis, using a logistic regression analysis with backward elimination. To evaluate the contribution of a parameter to the prediction of false negative results, the area under the curve (A_z) values were compared by receiver-operating-characteristic (ROC) curve analysis. A P value of less than 0.05 was considered statistically significant. All statistical analyses were performed with SPSS software (version 23.0, IBM).

Table 4
Assessment of pretreatment MR imaging features correlated with pathological response.

	All patients	pCR	False negative	P value
Multifocal or multicentric disease				0.192
Absent	171 (81.8)	92 (85.2)	79 (78.2)	
Present	38 (18.2)	16 (14.8)	22 (21.8)	
Background parenchymal enhancement				0.640
Minimal or mild	169 (80.9)	86 (79.6)	83 (82.2)	
Moderate or marked	40 (19.1)	22 (20.4)	18 (17.8)	
Type of lesion				0.015
Mass	192 (91.9)	104 (96.3)	88 (87.1)	
NME	17 (8.1)	4 (3.7)	13 (12.9)	
Mass shape				0.009
Oval or round	40 (20.8)	29 (27.9)	11 (12.5)	
Irregular	152 (79.2)	75 (72.1)	77 (87.5)	
Mass margin				0.189
Circumscribed	19 (9.9)	13 (12.5)	6 (6.8)	
Not circumscribed	173 (90.1)	91 (87.5)	82 (93.2)	
Mass internal enhancement				0.954
Heterogeneous	148 (77.1)	80 (76.9)	68 (77.3)	
Rim enhancement	44 (22.9)	24 (23.1)	20 (22.7)	
Mass peritumoral edema				0.417
Absent	114 (59.4)	59 (56.7)	55 (62.5)	
Present	78 (40.6)	45 (43.3)	33 (37.5)	
Mass intratumoral high signal on T2WI				0.871
Absent	121 (63.0)	65 (62.5)	56 (63.6)	
Present	71 (37.0)	39 (37.5)	32 (36.4)	
NME distribution				0.294
Segmental	8 (47.1)	3 (75)	5 (38.5)	
Regional	9 (52.9)	1 (25)	8 (61.5)	
NME internal enhancement				0.261
Heterogeneous	12 (70.6)	4 (100)	8 (61.5)	
Clumped	5 (29.4)	0 (0)	5 (38.5)	
CAD-generated kinetics				
Tumor diameter*	3.6 ± 1.7	3.4 ± 1.5	3.9 ± 1.8	0.024
Angio volume (cm^3)*	12.6 ± 18.1	12.5 ± 17.7	12.8 ± 19.2	0.312
Peak enhancement*	334.8 ± 219.8	330.9 ± 226.5	345.0 ± 202.6	0.024
Persistent component (%)*	40.6 ± 20.0	37.6 ± 19.1	43.8 ± 20.6	0.024
Plateau component (%)*	32.4 ± 10.6	32.9 ± 11.2	31.8 ± 10.1	0.462
Washout component (%)*	26.8 ± 17.6	29.5 ± 17.6	24.0 ± 17.3	0.024
Kinetic curve presented by CAD				> 0.999
Delayed plateau pattern	3 (1.4)	2 (1.9)	1 (1)	
Delayed washout pattern	206 (98.6)	106 (98.1)	100 (99)	

Note: Data are number of patients, with percentages in parentheses. CAD = computer-aided diagnosis, NME = non-mass enhancement, pCR = pathologic complete response, T2WI = T2-weighted image.
* Data are means ± standard deviations.

3. Results

3.1. Study population and tumor characteristics

Of the originally selected 250 patients, 31 met the exclusion criteria as follows: diagnosis and pretreatment MR imaging performed at a different institution without recorded information on the use of a computer-aided diagnosis (CAD) system (n = 21); bilateral breast cancer (n = 6); distant metastasis at the time of diagnosis (n = 2); underwent neoadjuvant endocrine therapy (n = 2). Table 1 describes the patient and disease characteristics of the 209 women identified as showing rCR that were included in this study. Of them, 108/209 (51.7%) also showed pCR, whereas 101/209 (48.3%) demonstrated residual lesion upon surgical histopathology (i.e. a false-negative rCR). In total, 18/209 (8.6%) received an anthracycline-based regimen, 178/209 (85.2%) received an anthracycline- and taxane-based regimen, and 13/209 (6.2%) received a HER2-targeted regimen with anthracycline- and taxane-based regimen. There were no significant differences in clinical stage at diagnosis or NAC regimen between the pCR and false-negative groups.

False-negative findings were significantly more frequent in patients with 1 or 2 histologic grade ($p = 0.001$), low tumor-infiltrating lymphocyte counts ($p = 0.004$), positive for ER ($p < 0.001$), positive for PR ($p < 0.001$), low Ki-67 ($p = 0.002$), luminal A or B subtype ($p < 0.001$) and a post-NAC mastectomy ($p < 0.001$).

3.2. Relationships between imaging features and false-negative findings

Mammographic features and changes in calcifications that were significantly and positively associated with false-negative results included lesions with calcifications ($p = 0.002$) and irregular shape ($p = 0.02$) (Table 2). Neither the morphology or distribution of pre-NAC calcifications nor the changes after NAC differed significantly between groups.

US features that were significantly more common in false negatives included non-mass lesions ($p = 0.015$) and spiculated margin ($p = 0.041$) (Table 3). The finding of an irregular shape on US was not significantly different between groups.

Upon analyzing MR imaging data regarding pretreatment morphology and kinetic assessment, significant positive correlations were found between false-negative rCR results and non-mass enhancement ($p = 0.015$), irregular shape ($p = 0.009$), large tumor diameter ($p = 0.024$), high peak enhancement ($p = 0.024$), a high proportion of the persistent component ($p = 0.024$), and finally, a low proportion of the washout component ($p = 0.024$) (Table 4).

Univariate logistic regression analysis identified significant associations of false negatives with: 1) lesions with calcifications (odds ratio [OR], 2.41 [95% confidence interval (CI): 1.37–4.25], $p = 0.002$) and

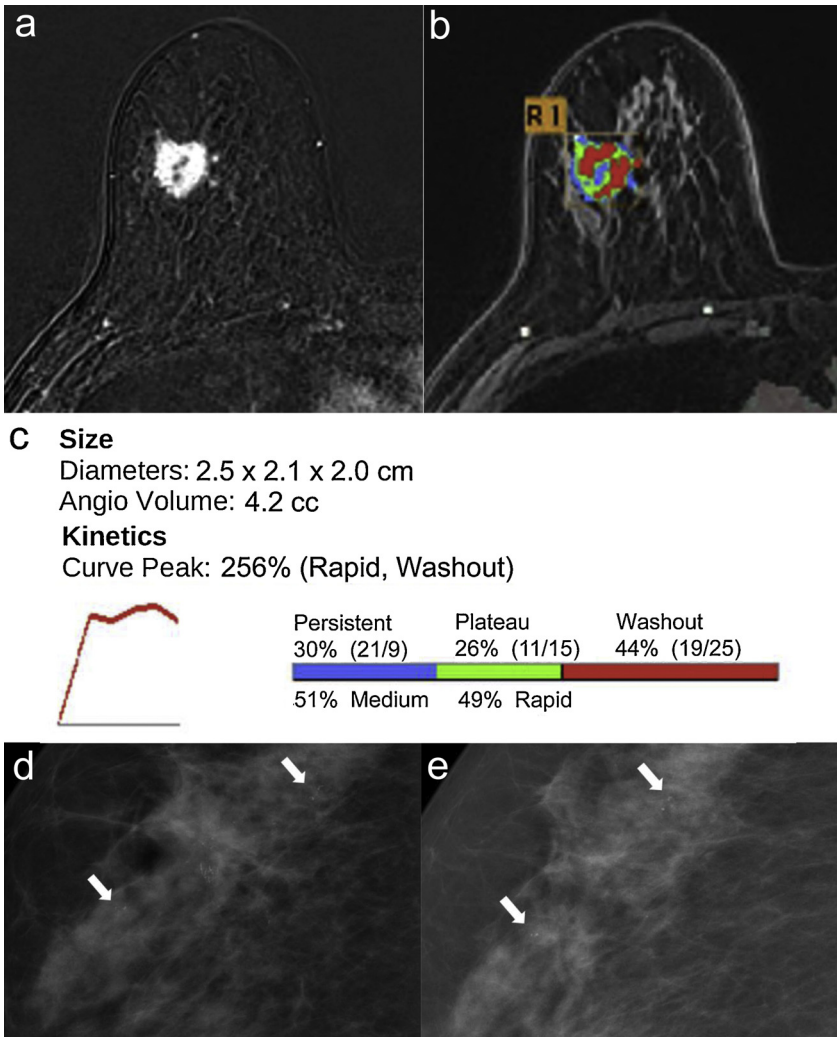

Fig. 1. 59-year-old woman with HER2-positive cancer who demonstrated pathologic complete response.
A, **B**, The pretreatment axial fat-suppressed T1-weighted contrast-enhanced MR image and MR image with CAD color overlay map shows a round shape, rim enhancing mass with tumor enhancement kinetics. **C**, Kinetic curve graph showing 44% of delayed washout component. **D**, Pretreatment mammography shows a 2.0 cm mass with an associated 6.5 cm malignant calcification. **E**, Post-treatment mammography shows a decreased size and number of malignant mass and calcifications, respectively. No invasive and in situ cancer was seen at histologic examination, thereby enabling us to confirm a pathologic complete response.

irregular shape (OR, 2.56 [95% CI: 1.14–5.73, $p = 0.023$) in mammography; 2) non-mass lesion (OR, 3.84 [95% CI: 1.21–12.20, $p = 0.015$) and spiculated margin (OR, 2.03 [95% CI: 1.02–4.02, $p = 0.043$) in US; and 3) multifocal multicentric lesion (OR, 2.40 [95% CI: 1.37–4.22, $p = 0.002$), non-mass enhancement (OR, 3.84 [95% CI: 1.21–12.20, $p = 0.023$), irregular shape (OR, 2.71 [95% CI: 1.26–5.81, $p = 0.011$), large tumor diameter (OR, 1.21 [95% CI: 1.02–1.44, $p = 0.026$), a high proportion of persistent component (OR, 1.02 [95% CI: 1.00–1.03, $p = 0.026$), and a low proportion of washout component (OR, 1.02 [95% CI: 1.00–1.03, $p = 0.025$) in MR imaging.

Multivariate analysis of radiologic findings in all patients identified significant, independent associations of false negatives with calcifications in mammography (OR, 1.88 [95% CI: 1.04–3.41], $p = 0.037$), multifocal multicentric lesion (OR, 2.42 [95% CI: 1.34–4.37, $p = 0.004$) and non-mass enhancement in MR imaging (OR, 4.06 [95% CI: 1.21–13.60], $p = 0.023$). Examples of patients with pCR and false-negative findings are provided in Figs. 1 and 2.

The A_z values of each parameters were 0.61 (95% CI, 0.53–0.68) for calcification in mammography, 0.54 (95% CI, 0.46–0.61) for multifocal multicentric lesion, and 0.55 (95% CI, 0.47–0.62) for type of lesion in MR imaging (Fig. 3). The A_z value for combined MR features was 0.57 (95% CI, 0.50–0.65) and combined all features including mammography and MR features was 0.64 (95% CI, 0.56–0.71).

4. Discussion

In our study, calcifications in mammography, multifocal multicentric lesions, and non-mass enhancement in pretreatment MR imaging were significant independent factors in predicting false-negative findings after NAC of breast cancer patients with rCR in MR imaging.

Many researchers have reported the importance of pCR and the improved long-term outcome [6–8,25]. In the preoperative neoadjuvant setting, accurate information from radiologic imaging on whether there is residual malignancy present or whether pCR is required may be important in guiding surgical management or avoiding unnecessary surgery. The definition of pCR may differ according to the presence of DCIS or residual lymph nodes after surgery. pCR, defined as demonstrating no invasive and no in situ residuals in breast and nodes, is the best discriminator between favorable and unfavorable patient outcomes, especially in more aggressive breast cancer subtypes [25,26]. Moreover, when trying to avoid surgery for women with rCR in MR imaging [19,27], it is crucial that the DCIS component is taken into account, as residual DCIS needs to be completely excised to minimize the risk of subsequent local recurrence. We defined pCR as the absence of residual invasive cancer or DCIS in the breast.

Marinovich et al. [10] found that MR imaging accuracy changed significantly depending on the pCR definition used, such that including a lack of DCIS in the definition of pCR would reduce false-positive cases. In our study, 42.6% (43/101) of false-negative cases had only residual DCIS. MR imaging is less sensitive when detecting DCIS relative to invasive carcinoma and calcifications seen on preoperative mammography which may represent the total tumor burden. In our study, 30.6% (33/108) of pCR cases and 51.5% (52/101) of false-

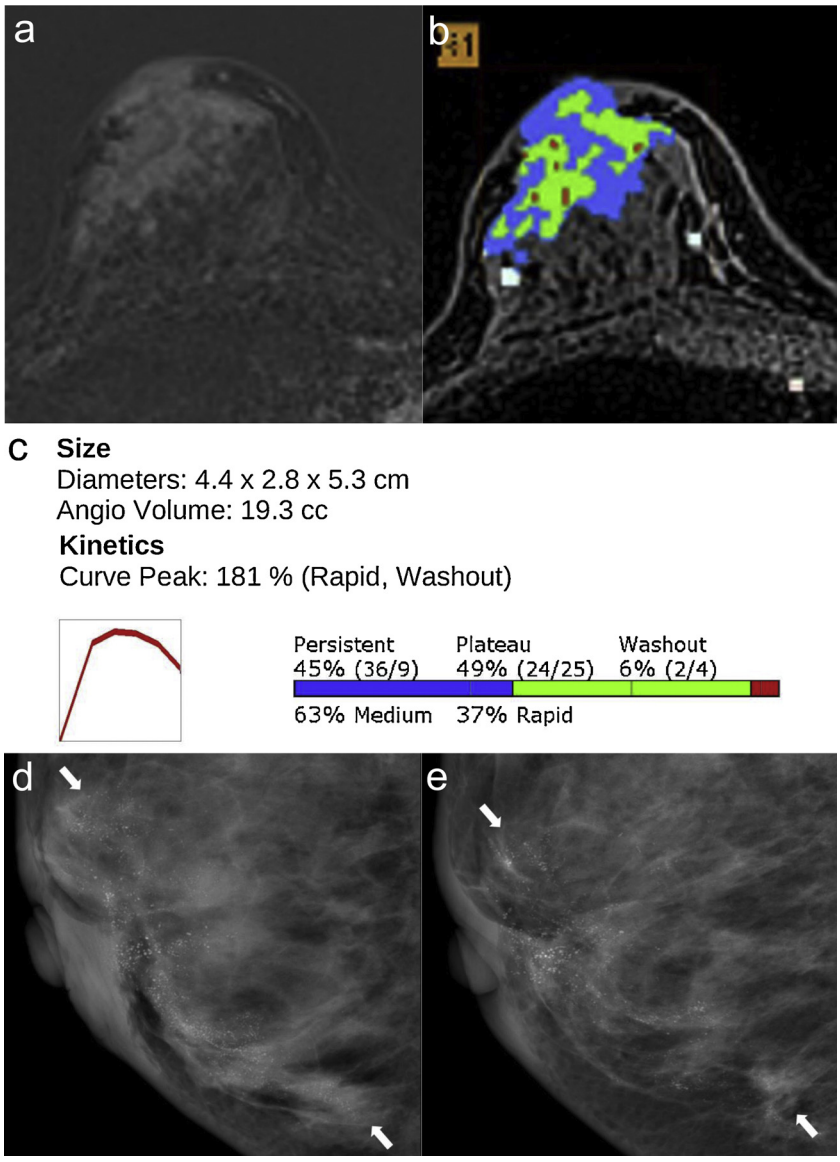

Fig. 2. 37-year-old woman with luminal A subtype breast cancer with a false-negative MR imaging result.
A, **B**, The pretreatment axial fat-suppressed T1-weighted contrast-enhanced MR image and MR image with CAD color overlay map shows regional distributed, heterogenous non-mass enhancement with tumor enhancement kinetics. **C**, Kinetic curve graph showing 6% of delayed washout component. **D**, Pretreatment mammography shows 7.5 cm asymmetry with malignant calcification. **E**, Post-treatment mammography shows decreased asymmetry with no change in malignant calcification. Surgical histology revealed a 6.8 cm residual invasive ductal carcinoma.

negative cases had calcifications in mammography. In fact this feature was a significant independent factor for false-negative findings; however, the morphology, distribution or changes in calcifications did not show significant differences. This result is consistent with previous studies [28–30] indicating that residual microcalcifications may represent remnant malignancy, but may instead be necrotic tissue in which the cancer cells die and release calcium after treatment [28–32]. An et al. [29] reported 44.8% of residual microcalcifications did not correlate with residual malignancy, while the extent of residual microcalcifications as measured by mammography were in poor agreement with the size of pathologically determined residual tumors. Adrada et al. [28] found that the extent of calcifications on mammography following NAC did not correlate with the extent of residual disease in up to 22% of women, and no correlation existed between changes in the extent of calcifications before and after NAC and pCR. Feliciano et al. [17] reported that all microcalcifications within the tumor bed should be completely excised, although not all of the residual microcalcifications on post-NAC mammograms will reflect residual malignancy. Persistence of microcalcifications does not necessarily indicate the presence of DCIS, thus evaluating residual microcalcifications on mammography remains an area of difficulty in the interpretation while evaluating the response in patients who have undergone NAC. Moreover, the A_z value was 0.61 for calcification in mammography, 0.57 for combined MR features and increased to 0.64 in the combination of all features including mammography and MR features. Both mammography and MR imaging may have important roles for the final assessment before surgery especially in patients with calcifications.

According to the molecular subtype, pCR was most frequent for triple-negative breast cancer (42.6%, 46/108). False-negative findings were significantly more frequent in both luminal A and B subtypes with 1 or 2 histologic grades. These findings are consistent with published results reporting higher pCR for ER-negative tumors [13,28]. Los Santos et al. [9] found that the negative predictive value was highest for patients who had hormone negative, HER2-positive and triple-negative breast cancers, but it was still only in the 60% range. They confirmed that among patients who achieved rCR in MR imaging, positive hormone status, and low tumor grade were most commonly associated with residual disease at surgery. Namura et al. [33] also reported that ER-positive, HER2-negative breast cancer had the lowest negative predictive value, while ER-negative subtypes had high negative predictive values regardless of HER2 amplification. Chen et al. [34] demonstrated higher false-negative rates and larger size discrepancies in HER2-negative breast cancer; they also noted that non-mass

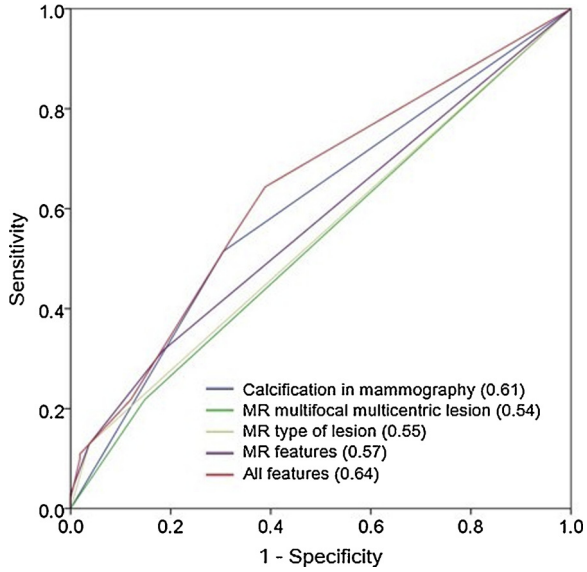

Fig. 3. Receiver-operating characteristics curve for the prediction of false negative results. The A_z values for the combined MR features was 0.57 and combined all features was 0.64.

enhancement is more likely to show residual disease as small foci or scattered cells after NAC, leading to an underestimation of the residual disease extent at MR imaging. This is consistent with our finding that non-mass enhancement at MR imaging is an independent factor for false-negative results.

This study has several limitations. First, this was a retrospective single-center study using various chemotherapy regimens and different cycles before surgery. Second, the imaging review was done retrospectively and had potentially high inter- and intra-observer variability. Finally, we did not evaluate the prognoses of the patients and suggest an analysis of disease-free survival rates should be included in a future study.

5. Conclusion

In conclusion, patients with calcification in mammography, multifocal multicentric lesions, and non-mass enhancement in pretreatment MR imaging are significantly associated with false-negative results who showed rCR on MR imaging after NAC. These patient populations should be interpreted with caution.

Acknowledgement

None.

References

[1] J.S. Mieog, J.A. van der Hage, C.J. van de Velde, Neoadjuvant chemotherapy for operable breast cancer, Br. J. Surg. 94 (2007) 1189–1200, https://doi.org/10.1002/bjs.5894.

[2] J.R. Gralow, H.J. Burstein, W. Wood, G.N. Hortobagyi, L. Gianni, G. von Minckwitz, A.U. Buzdar, I.E. Smith, W.F. Symmans, B. Singh, E.P. Winer, Preoperative therapy in invasive breast cancer: pathologic assessment and systemic therapy issues in operable disease, J. Clin. Oncol. 26 (2008) 814–819, https://doi.org/10.1200/JCO.2007.15.3510.

[3] M. Kaufmann, G. von Minckwitz, H.D. Bear, A. Buzdar, P. McGale, H. Bonnefoi, M. Colleoni, C. Denkert, W. Eiermann, R. Jackesz, A. Makris, W. Miller, J.Y. Pierga, V. Semiglazov, A. Schneeweiss, R. Souchon, V. Stearns, M. Untch, S. Loibl, Recommendations from an international expert panel on the use of neoadjuvant (primary) systemic treatment of operable breast cancer: new perspectives 2006, Ann. Oncol. 18 (2007) 1927–1934, https://doi.org/10.1093/annonc/mdm201.

[4] A. Ring, A. Webb, S. Ashley, W.H. Allum, S. Ebbs, G. Gui, N.P. Sacks, G. Walsh, I.E. Smith, Is surgery necessary after complete clinical remission following neoadjuvant chemotherapy for early breast cancer? J. Clin. Oncol. 21 (2003) 4540–4545, https://doi.org/10.1200/JCO.2003.05.208.

[5] S. Kummel, J. Holtschmidt, S. Loibl, Surgical treatment of primary breast cancer in the neoadjuvant setting, Br. J. Surg. 101 (2014) 912–924, https://doi.org/10.1002/bjs.9545.

[6] P. Rastogi, S.J. Anderson, H.D. Bear, C.E. Geyer, M.S. Kahlenberg, A. Robidoux, R.G. Margolese, J.L. Hoehn, V.G. Vogel, S.R. Dakhil, D. Tamkus, K.M. King, E.R. Pajon, M.J. Wright, J. Robert, S. Paik, E.P. Mamounas, N. Wolmark, Preoperative chemotherapy: updates of national surgical adjuvant breast and bowel project protocols B-18 and B-27, J. Clin. Oncol. 26 (2008) 778–785, https://doi.org/10.1200/JCO.2007.15.0235.

[7] W.F. Symmans, F. Peintinger, C. Hatzis, R. Rajan, H. Kuerer, V. Valero, L. Assad, A. Poniecka, B. Hennessy, M. Green, A.U. Buzdar, S.E. Singletary, G.N. Hortobagyi, L. Pusztai, Measurement of residual breast cancer burden to predict survival after neoadjuvant chemotherapy, J. Clin. Oncol. 25 (2007) 4414–4422, https://doi.org/10.1200/JCO.2007.10.6823.

[8] X. Kong, M.S. Moran, N. Zhang, B. Haffty, Q. Yang, Meta-analysis confirms achieving pathological complete response after neoadjuvant chemotherapy predicts favourable prognosis for breast cancer patients, Eur. J. Cancer 47 (2011) 2084–2090, https://doi.org/10.1016/j.ejca.2011.06.014.

[9] J.F. De Los Santos, A. Cantor, K.D. Amos, A. Forero, M. Golshan, J.K. Horton, C.A. Hudis, N.M. Hylton, K. McGuire, F. Meric-Bernstam, I.M. Meszoely, R. Nanda, E.S. Hwang, Magnetic resonance imaging as a predictor of pathologic response in patients treated with neoadjuvant systemic treatment for operable breast cancer: translational breast cancer research consortium trial 017, Cancer 119 (2013) 1776–1783, https://doi.org/10.1002/cncr.27995.

[10] M.L. Marinovich, N. Houssami, P. Macaskill, F. Sardanelli, L. Irwig, E.P. Mamounas, G. von Minckwitz, M.E. Brennan, S. Ciatto, Meta-analysis of magnetic resonance imaging in detecting residual breast cancer after neoadjuvant therapy, J. Natl. Cancer Inst. 105 (2013) 321–333, https://doi.org/10.1093/jnci/djs528.

[11] Y.L. Gu, S.M. Pan, J. Ren, Z.X. Yang, G.Q. Jiang, Role of magnetic resonance imaging in detection of pathologic complete remission in breast cancer patients treated with neoadjuvant chemotherapy: a meta-analysis, Clin. Breast Cancer 17 (2017) 245–255, https://doi.org/10.1016/j.clbc.2016.12.010.

[12] Y. Yuan, X.S. Chen, S.Y. Liu, K.W. Shen, Accuracy of MRI in prediction of pathologic complete remission in breast cancer after preoperative therapy: a meta-analysis, AJR Am. J. Roentgenol. 195 (2010) 260–268, https://doi.org/10.2214/AJR.09.3908.

[13] W.J. Choi, W.K. Kim, H.J. Shin, J.H. Cha, E.Y. Chae, H.H. Kim, Evaluation of the tumor response after neoadjuvant chemotherapy in breast cancer patients: correlation between dynamic contrast-enhanced magnetic resonance imaging and pathologic tumor cellularity, Clin. Breast Cancer 18 (2018) e115–e121, https://doi.org/10.1016/j.clbc.2017.08.003.

[14] N.L. Eun, H.M. Gweon, E.J. Son, J.H. Youk, J.A. Kim, Pretreatment MRI features associated with diagnostic accuracy of post-treatment MRI after neoadjuvant chemotherapy, Clin. Radiol. 73 (2018), https://doi.org/10.1016/j.crad.2018.02.008 676 e679–676 e614.

[15] B.B. Choi, S.H. Kim, Effective factors to raise diagnostic performance of breast MRI for diagnosing pathologic complete response in breast cancer patients after neoadjuvant chemotherapy, Acta Radiol. 56 (2015) 790–797, https://doi.org/10.1177/0284185114538622.

[16] M.B. Lobbes, R. Prevos, M. Smidt, V.C. Tjan-Heijnen, M. van Goethem, R. Schipper, R.G. Beets-Tan, J.E. Wildberger, The role of magnetic resonance imaging in assessing residual disease and pathologic complete response in breast cancer patients receiving neoadjuvant chemotherapy: a systematic review, Insights Imaging 4 (2013) 163–175, https://doi.org/10.1007/s13244-013-0219-y.

[17] Y. Feliciano, A. Mamtani, M. Morrow, M.M. Stempel, S. Patil, M.S. Jochelson, Do calcifications seen on mammography after neoadjuvant chemotherapy for breast cancer always need to be excised? Ann. Surg. Oncol. 24 (2017) 1492–1498, https://doi.org/10.1245/s10434-016-5741-y.

[18] J. Heil, S. Kummel, B. Schaefgen, S. Paepke, C. Thomssen, G. Rauch, B. Ataseven, R. Grosse, V. Dreesmann, T. Kuhn, S. Loibl, J.U. Blohmer, G. von Minckwitz, Diagnosis of pathological complete response to neoadjuvant chemotherapy in breast cancer by minimal invasive biopsy techniques, Br. J. Cancer 113 (2015) 1565–1570, https://doi.org/10.1038/bjc.2015.381.

[19] J. Heil, B. Schaefgen, P. Sinn, H. Richter, A. Harcos, C. Gomez, A. Stieber, A. Hennigs, G. Rauch, F. Schuetz, C. Sohn, A. Schneeweiss, M. Golatta, Can a pathological complete response of breast cancer after neoadjuvant chemotherapy be diagnosed by minimal invasive biopsy? Eur. J. Cancer 69 (2016) 142–150, https://doi.org/10.1016/j.ejca.2016.09.034.

[20] G.M. Rauch, H.M. Kuerer, B. Adrada, L. Santiago, T. Moseley, R.P. Candelaria, E. Arribas, J. Sun, J.W.T. Leung, S. Krishnamurthy, W.T. Yang, Biopsy feasibility trial for breast cancer pathologic complete response detection after neoadjuvant chemotherapy: imaging assessment and correlation endpoints, Ann. Surg. Oncol. 25 (2018) 1953–1960, https://doi.org/10.1245/s10434-018-6481-y.

[21] H. Kim, H.H. Kim, J.S. Park, H.J. Shin, J.H. Cha, E.Y. Chae, W.J. Choi, Prediction of pathological complete response of breast cancer patients undergoing neoadjuvant chemotherapy: usefulness of breast MRI computer-aided detection, Br. J. Radiol. 87 (2014) 20140142, https://doi.org/10.1259/bjr.20140142.

[22] T.C. Williams, W.B. DeMartini, S.C. Partridge, S. Peacock, C.D. Lehman, Breast MR imaging: computer-aided evaluation program for discriminating benign from malignant lesions, Radiology 244 (2007) 94–103, https://doi.org/10.1148/radiol.2441060634.

[23] American College of Radiology, BI-RADS Committee, ACR BI-RADS Atlas Breast Imaging and Reporting Data System, 5th ed., American College of Radiology, Reston, VA, 2013.

[24] A. Goldhirsch, W.C. Wood, A.S. Coates, R.D. Gelber, B. Thurlimann, H.J. Senn, M. Panel, Strategies for subtypes–dealing with the diversity of breast cancer:

highlights of the St. Gallen international expert consensus on the primary therapy of early breast cancer 2011, Ann. Oncol. 22 (2011) 1736–1747, https://doi.org/10.1093/annonc/mdr304.
[25] G. von Minckwitz, M. Untch, J.U. Blohmer, S.D. Costa, H. Eidtmann, P.A. Fasching, B. Gerber, W. Eiermann, J. Hilfrich, J. Huober, C. Jackisch, M. Kaufmann, G.E. Konecny, C. Denkert, V. Nekljudova, K. Mehta, S. Loibl, Definition and impact of pathologic complete response on prognosis after neoadjuvant chemotherapy in various intrinsic breast cancer subtypes, J. Clin. Oncol. 30 (2012) 1796–1804, https://doi.org/10.1200/JCO.2011.38.8595.
[26] G. von Minckwitz, M. Untch, S. Loibl, Update on neoadjuvant/preoperative therapy of breast cancer: experiences from the German breast group, Curr. Opin. Obstet. Gynecol. 25 (2013) 66–73, https://doi.org/10.1097/GCO.0b013e32835c0889.
[27] R.F. van la Parra, H.M. Kuerer, Selective elimination of breast cancer surgery in exceptional responders: historical perspective and current trials, Breast Cancer Res. 18 (2016) 28, https://doi.org/10.1186/s13058-016-0684-6.
[28] B.E. Adrada, L. Huo, D.L. Lane, E.M. Arribas, E. Resetkova, W. Yang, Histopathologic correlation of residual mammographic microcalcifications after neoadjuvant chemotherapy for locally advanced breast cancer, Ann. Surg. Oncol. 22 (2015) 1111–1117, https://doi.org/10.1245/s10434-014-4113-8.
[29] Y.Y. An, S.H. Kim, B.J. Kang, Residual microcalcifications after neoadjuvant chemotherapy for locally advanced breast cancer: comparison of the accuracies of mammography and MRI in predicting pathological residual tumor, World J. Surg. Oncol. 15 (2017) 198, https://doi.org/10.1186/s12957-017-1263-8.
[30] S.J. Vinnicombe, A.D. MacVicar, R.L. Guy, J.P. Sloane, T.J. Powles, G. Knee, J.E. Husband, Primary breast cancer: mammographic changes after neoadjuvant chemotherapy, with pathologic correlation, Radiology 198 (1996) 333–340, https://doi.org/10.1148/radiology.198.2.8596827.
[31] A. Weiss, K.C. Lee, Y. Romero, E. Ward, Y. Kim, H. Ojeda-Fournier, J. Einck, S.L. Blair, Calcifications on mammogram do not correlate with tumor size after neoadjuvant chemotherapy, Ann. Surg. Oncol. 21 (2014) 3310–3316, https://doi.org/10.1245/s10434-014-3914-0.
[32] L.E. Esserman, M. d'Almeida, D. Da Costa, D.M. Gerson, R.J. Poppiti Jr., Mammographic appearance of microcalcifications: can they change after neoadjuvant chemotherapy? Breast J. 12 (2006) 86–87, https://doi.org/10.1111/j.1075-122X.2006.00195.x.
[33] M. Namura, H. Tsunoda, H. Yagata, N. Hayashi, A. Yoshida, E. Morishita, J. Takei, K. Suzuki, H. Yamauchi, Discrepancies between pathological tumor responses and estimations of complete response by magnetic resonance imaging after neoadjuvant chemotherapy differ by breast cancer subtype, Clin. Breast Cancer 18 (2018) 128–134, https://doi.org/10.1016/j.clbc.2017.07.001.
[34] J.H. Chen, S. Bahri, R.S. Mehta, A. Kuzucan, H.J. Yu, P.M. Carpenter, S.A. Feig, M. Lin, D.J. Hsiang, K.T. Lane, J.A. Butler, O. Nalcioglu, M.Y. Su, Breast cancer: evaluation of response to neoadjuvant chemotherapy with 3.0-T MR imaging, Radiology 261 (2011) 735–743, https://doi.org/10.1148/radiol.11110814.